JOURNAL OF ALGEBRAIC STATISTICS
Volume 13, No. 2, 2022, p. 3072-3083
https://publishoa.com
ISSN: 1309-3452

Machine Learning of Skin Cancer Diagnosis Based on Oriented FAST and Rotated BRIEFS

Muna Abdul Hussain Radhi[1], Khlood Ibraheem Abbas[2] , Rasha Shaker Ibrahim[3]

[1] Mustansiriyah University, College of Science, Computer Science Department Baghdad, Iraq, muna.ali@uomustansiriyah.edu.iq ; [2]Mustansiriyah University, College of Science, Computer Science Department Baghdad, Iraq, a.Khlood@uomustansiriyah.edu.iq;

[3]Mustansiriyah University, College of Science, Computer Science Department Baghdad, Iraq r.albadri@uomustansiriyah.edu.iq.

17/6/2022

Received 2022 March 25; **Revised** 2022 April 28; **Accepted** 2022 May 15.

ABSTRACT

Screening for malignant melanoma is critical to treating the disease and saving lives. Many computerized techniques have been reported in the literature to diagnose diseases and classify them with pathological performance to detect skin cancer. However, reducing the rate of misrepresentation remains a challenge and a concern, the use of false positives is worrying and requires intervention by an expert pathologist for further examination and examination. In this paper, an automated skin cancer diagnosis system that combines different properties that use new features in texture and color has been proposed in a distinctive bag approach for effective and accurate detection. To give good results, images must be processed by using an average filter in order to eliminate the noise that may occur in the image, so we need to highlight the affected part, so it is isolated through the watershed method and then the affected part is distinguished using the colored skin lesion hash algorithm that teaches representative texture distributions and calculates the texture excellence scale for each distribution. A fabric vector is extracted for each pixel in the image. Powerful features are then extracted using the ORB method. Finally, to give good results, one method of machine learning is SVM, which is one of the distinct ways of efficiency, speed and accuracy compared to other methods. The system was trained and tested at 30% of the HAM10,000 data set used, so when calculating the system's assessment of skin cancer, it was discovered that the results were excellent, with 98% accuracy, 95% sensitivity, and 96% privacy, meaning that the system works accurately and efficiently.

Keywords: skin cancer, medium filter, Watershed segmentation, ORB, SVM.

1. Introduction

Becautilize the skin is the body's biggest organ, the impacts of different viral, bacterial, and inflammatory diseases travel throughout the body, cautilizing a wide range of health problems. As depicted in Figure (1), skin illnesses include acne, atopic dermatitis, alopecia, morphea, melanoma, photoaging, wounds, psoriasis, wrinkles, and vitiligo. Many of these diseases can be healed if they are caught early enough before they spread. Dermoscopy is a procedure that utilizes polarization to minimize surface reflection and is utilized by professionals to study skin changes with the utilize of strong light. Around the world, more than 100 million people suffer from various types of skin illnesses. Skin cancer is also on the rise, and there aren't many cures available. Melanoma is the deadliest as well as the most diverse kind of skin cancer among them. Early-stage studies can aid in preventing the spread of skin disease. The goal of this research is to develop a novel dynamic graph cut technique for segmenting the damaged skin patches, followed by a probabilistic classifier for identifying the skin disease kind. When compared to other image segmentation methods, the graph cut approach offers superior accuracy and performance [1-6]. Conversely, Nave Bayes classifiers are extremely simple, and they converge faster than other comparable discriminative models such as logistic regression, utilizing less training data. Skin cancer is the sixth most common kind of cancer in the world, and its rates are rising. Skin is made up of cells, and these cells make

JOURNAL OF ALGEBRAIC STATISTICS
Volume 13, No. 2, 2022, p. 3072-3083
https://publishoa.com
ISSN: 1309-3452

up tissues. As, a result, cancer is produced by aberrant or uncontrolled cell proliferation in the related tissues or other neighboring tissues. Cancer may be cautilized by UV light exposure, a weakened immune system, a family history, and other factors. This type of atypical cell growth pattern can be classified as benign or cancerous. Benign tumors are cancerous tumors that are usually considered harmless moles. On the other hand, malignant tumors are treated as life-threatening cancers. It can also damage other body tissues. Basal cells, squamous cells and melanocytes are the three types of cells that make up the upper layer of the skin. These are the ones who make the tissue malignant. Skin malignant tumors come in a variety of forms, with skin cancer, basal cell carcinoma (BCC) and squamous cell carcinoma (SCC) the most threatening. The intimacy of pigment cells, intersectoral curvature (AK), benign curvature, skin fibroids, and vascular lesions are among other forms. Skin cancer is the most serious cancer, can return even after it is removed. Skin cancer is most prevalent in Australia and the United States [7-9].

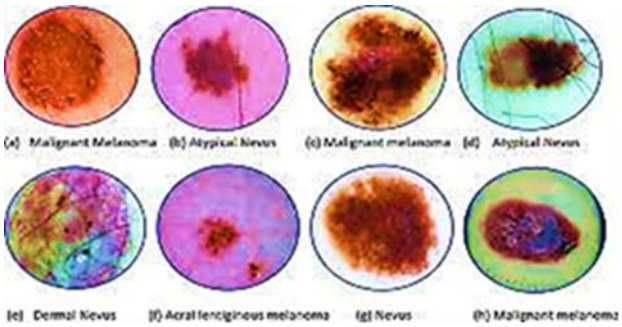

Figure (1) skin cancer

2. Literature Review

The variety of research that has been utilized in Machine Learning of Skin Cancer Diagnosis will be discussed in this paragraph, as shown below.:

On the SD-198 dataset, we utilized a representation inspired by To diagnose clinical skin lesions, utilize the ABCD rule. Compare procedures recommended by dermatologists with deep learning techniques. Accuracy was 57.62 percent, compared to 53.35 ppercentfor the best deep learning technology (ResNet). Compared to other doctors, only senior doctors with significant experience in dermatology were offered an average accuracy of 83.29 percent [10].

Faced the challenge of diagnosing clinical skin lesions, which is more challenging than finding skin cancer on laparoscopic skin images. We want to see if computers can measure the diagnostic criteria used by doctors. We propose six discriminatory and interpretable representations of the diagnosis of skin lesions using acceptable skin standards. In a standard data set, experiments suggest that both low-level and deep features outperform the proposed representations. Furthermore, dermatologists agree that the final results on clinical images with 198 categories of dermatology are comparable have been presented [11].

Claim that the Gradient Chart (HG) and the Line Chart (HL) are better for analyzing and classifying laparoscopic and standard skin images than the traditional guided gradient chart (HOG) and the guided line chart (HOL), respectively. To take advantage of color information, HG and HL are independently filled using a code book and combined with additional packed color vector angles and Zernike moments. Extensive tests with different works were used on a endoscopic image data set and a standard data set to evaluate the entire system. The proposed system outperformed the latest methods of experimentation, demonstrating its superiority has been presented [12].

The best feature for deep learning and extreme learning machine is used to offer a new technique for classifying multilayered skin lesions. Get images and improve contrast; extract deep learning with transformative learning; best choose features using hybrid whale optimization and intertropy information approach (EMI); integrate selected features using a modified basic link-based approach; and finally, the extreme learning machine-based classification is the five basic steps in the proposed method. The selection phase of features increases computational efficiency and system accuracy. HAM10,000 and ISIC2018 are publicly available data sets used in the experiment. In both data sets, accuracy was 93.40

JOURNAL OF ALGEBRAIC STATISTICS
Volume 13, No. 2, 2022, p. 3072-3083
https://publishoa.com
ISSN: 1309-3452

per cent and 94.36 per cent, respectively. The proposed strategy outperforms the latest methods (SOTA) in terms of accuracy. Moreover, the proposed technology is effective in terms of computing has been presented [13].

Using a deep bypass neural network, a new automated technique for identifying and identifying skin lesions (DCNN) has been developed. The proposed cascading design includes three basic steps: a) improving contrast using the local Rapid Local Lablastic Filtration (FlLpF) and converting HSV color. b) Extract pest boundaries using CNN and XOR colored playback; and c) extract in-depth features using transitional learning and inception V3 model before integrating features using the Connectivity Distance Method (HD). To choose the most distinctive features, choose an entropy-controlled feature have been presented [14].

Utilizing deep learning-based methodologies to automate Training, with 50 percent remaining, 30 percent, and 10 percent serves as test groups. To extract the synthetic properties of the lesion, the statistical parameters of The Haarlik are calculated. GlCM common occurrence arrays are used with offsets of 2, 4, 8, 12, 16, 20, 24, 28, angle 0, 45, 90 and 135 degrees, respectively, to create these parameters. We determined the average, medium and standard deviation of the three color levels of the area of importance to extract color properties. These properties are inputs into the artificial neural network (ANN) for skin cancer screening. Haralik parameters and combined color characteristics have shown that they are superior to the features alone. experimentation based on another set of features often observed by dermatologists, such as asymmetry,Irregular borders, color and diameter (ABCD) have also been established. On the other hand, the "D" feature has been modified and renamed Oblongness. The length-to-width ratio is captured using this property. Furthermore, the use of modified standard deviation in conjunction with ABCD properties promotes the detection of skin cancer by 93.7 per cent have been presented [15].

3.Oriented FAST and Rotated BRIEF (ORB)

At OpenCV Laboratories in 2011, Ethan Robley, Vincent Rabo, Kurt Connolage and Gary R. Bradsky developed Fast Waver and Rotor Summary (ORB) as an effective and practical alternative to SIFT and SURF. ORB is designed because SIFT and SURF are patented algorithms.

In terms of discovering features, ORB bypass sift (and SURF) despite being almost two ranks faster. The ORB descriptor relies on the FAST key point detector, which is known. Due to its high efficiency and low cost, both techniques are desirable. ORB's main contributions are as follows::

- FAST now includes a fast and accurate steering component.
- Calculate brief properties effectively oriented
- Analysis of contrast and correlation between BRIEF-oriented properties
- A tutorial approach to decorating BRIEF features while maintaining rotational stability, improving performance in nearby applications.

3.1 Fast(Features from Accelerated and Segments Test)

Fast compares the brightness of the p pixel in an array with the brightness of 16 pixels surrounding in a small circle around p. After that, pixels in the circle are divided into three groups (lighter than p, darker than p, or similar to p). It is chosen as a key point if it is darker or brighter than p by more than 8 pixels. As a result, fast's key points provide us with information about the location of the edges in the image. As shown in Figure (2).

JOURNAL OF ALGEBRAIC STATISTICS
Volume 13, No. 2, 2022, p. 3072-3083
https://publishoa.com
ISSN: 1309-3452

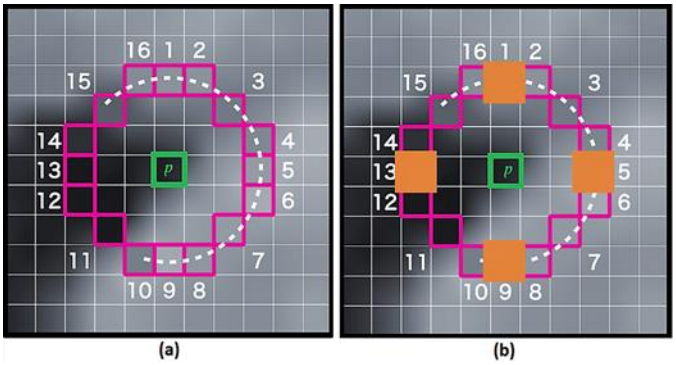

Figure(2) key point of FAST algorithm

FAST properties, on the other hand, lack a steering component and do not support multiple metrics. The orb algorithm uses a multi-metric pyramid of images. Multi-metric photography of a single image consists of many images, each of which is a different resolution version of the image, known as the image pyramid. Each level of the pyramid has a miniature version of the image from the previous level.

After forming a pyramid, Orb uses a quick approach to locate the main points in the image. Orb recognizes the key points in each level and correctly identifies the critical points on a different scale. In this sense, ORB is a constant measure.

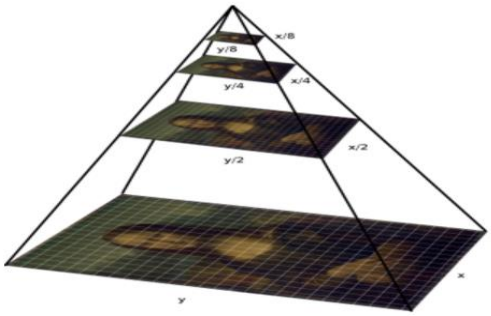

Figure (3) locating keypoints ORB

Depending on how density levels change at each crucial point, such as the left or right encounter, ORB assigns a direction. The orb uses centroid intensity to detect density variations. The centroid's in-tensity presupposes that the angle intensity is removed from the center, and this vector may be utilized to determine the direction.

To begin, the following are the characteristics of the corrective moments:

$$m_{pq} = \sum_{x,y} x^p y^q I(x,y) \quad \textbf{(1)}$$

With these moments, we may calculate the patch's centroid, or "center of mass," as follows:

$$C = \left(\frac{m_{10}}{m_{00}}, \frac{m_{01}}{m_{00}} \right) \quad \textbf{(2)}$$

We may make a vector from the corner's center O to the centroid -OC. The orientation of the patch is determined by the following:

$$\theta = \text{atan2}(m_{01}, m_{10}) \quad \textbf{(3)}$$

JOURNAL OF ALGEBRAIC STATISTICS
Volume 13, No. 2, 2022, p. 3072-3083
https://publishoa.com
ISSN: 1309-3452

Here's an example to help you understand the method:

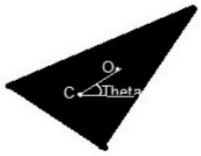

After computing the patch's orientation, we may rotate it to a canonical rotation and calculate the descriptor, resulting in rotation invariance.

3.2 BRIEF(Binary robust independent elementary feature)

BRIEF converts all of the relevant points found using the fast approach into a binary feature vector that may be used to represent an object. A binary feature vector (sometimes called a binary feature descriptor) is a feature vector that only contains the numbers 1 and 0. A feature vector, which is a 128–512 bit string, is used to represent each keypoint in a BRIEF.

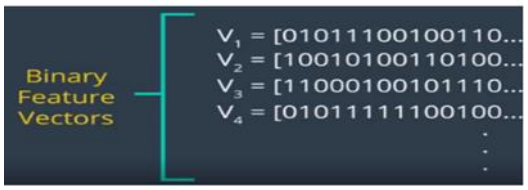

Figure (5) Binary Feature descriptor

To reduce the descriptor's ability to high frequency noise, BRIEF softens the image using a gaussy nucleus. BRIEF then selects a random pair of pixels from a pre-defined area surrounding that key point. The patch is a box of some pixel width and its height determines the specific neighborhood of the pixel. The first pixel is chosen in the random pair of Gausi distribution with the spread of the stranded Sigma centered around the main point. The second pixel in the random pair comes from a gausi distribution centered around the first pixel with a standard deviation or sigma dispersion by two. The trembling bit is set on 1 if the first pixel is brighter than the second; otherwise, it is set on 0.

BRIEF chooses a random pair and allocates a new value. To get a base point in a 128-bit vector, do this 128 times. Create a vector like this for each key point in an image. BRIEF, on the other hand, is not constant for rotation and is therefore used by ORB (conscious rotation summary). ORB includes these features while maintaining BRIEF speed.

Take a look at the smooth image correction below, p. The definition of binary testing is as follows:

$$\begin{aligned} &Where\,\tau(p;x,y)\,is\,defined\,as: \\ &\tau(p;x,y)=\begin{cases}1 & :p(x)<p(y)\\ 0 & :p(x)\geq p(y)\end{cases} \\ &p(x)\,is\,the\,\text{int}ensity\,value\,at\,pixel\,x. \end{aligned} \tag{4}$$

where p(x) denotes p's intensity at x. The feature is defined by a vector of n binary tests:

$$f(n)=\sum_{1<i<n}2^{i-1}\tau(p;x_i,y_i) \tag{5}$$

JOURNAL OF ALGEBRAIC STATISTICS
Volume 13, No. 2, 2022, p. 3072-3083
https://publishoa.com
ISSN: 1309-3452

BRIEF's matching performance plummets for in-plane rotations of more than a few degrees. ORB demonstrates a strategy for guiding BRIEF based on the orientation of the key-points. Any feature set of n binary tests at position (xi, yi) requires the 2 x n matrix:

$$S = \begin{pmatrix} x1,\dots x_n \\ y1,\dots y_n \end{pmatrix} \quad (6)$$

It creates a steered version S of S by combining the patch orientation with the rotation matrix R:

$$S_\theta = R_\theta S \quad (7)$$

As a result, the steered BRIEF operator's name has been changed to:

$$g_n(p,\theta) = f_n(p) \mid (x_i, y_i) \in S_\theta \quad (8)$$

The angle is then discretized into 2/30 (12 degree) increments, and a database of precomputed BRIEF patterns is created. The correct collection of points S will be used to compute its description as long as the keypoint orientation stays consistent between views.

4.The Proposal System

The system is fed a picture, which is subsequently pre-processed using the median filtering method. The preprocessed picture will be segmented using a watershed approach. The ORB program is then used to extract features from the segmented pictures. Finally, SVM is used to classify the data. Our proposed research structure is depicted in Figure (6).

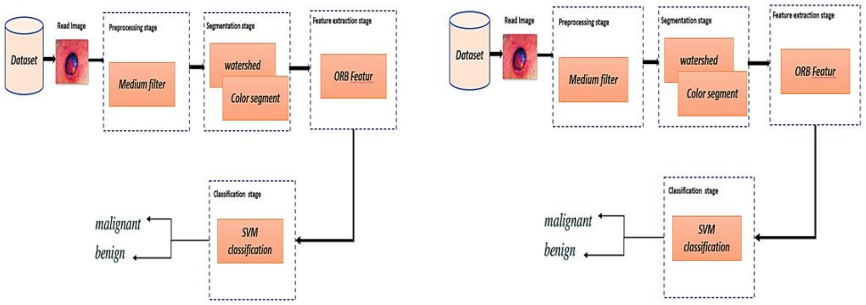

Figure (6) The proposal system of skin cancer

A. **Image Acquisition**

In every vision system, the initial stage is always image acquisition. Following the capturing of the picture, a variety of processing techniques may be used to perform a variety of image-related activities. Without a picture, processing is impossible, which is why acquiring an image is always the first step in a workflow sequence. Images may be collected in a number of ways, including using cameras and scanners. The captured image's properties must be kept in their entirety. Data for people with and without skin cancer was gathered for this paper, one of which was retrieved from the Kaggle Standard website.

1.Standard Dataset

The modest size and lack of diversity of available da-tasets of dermatoscopic images make it difficult to train machine learning for automated diagnosis of pigmented skin lesions. The HAM10000 ("Human Against Machine with 10000 training images") dataset addresses this is-sue. We gathered dermatoscopic images from various populations, which were

JOURNAL OF ALGEBRAIC STATISTICS
Volume 13, No. 2, 2022, p. 3072-3083
https://publishoa.com
ISSN: 1309-3452

captured and preserved utiliz-ing various modalities. 10015 dermatoscopic images make up the final dataset, which may be utilized as a training set for academic machine learning. The cases include a diverse range of pigmented lesions, including actinic keratoses and intraepithelial carcinoma / Bow-en's disease (akiec), basal cell carcinoma (bcc), benign keratosis-like lesions (solar lentigines / seborrheic ker-atoses and lichen-planus like keratoses, bkl), dermatofi-broma (df), melanom (angiomas, angiokeratomas, pyo-genic granulomas and hemorrhage, vasc). More than 50% of lesions are con-firmed by histopathology (histo); in the other cases, the ground truth is either follow-up investigation (follow up), expert consensus (consensus), or in-vivo confocal microscopy confirmation (confocal). The HAM10000 metadata file's lesion id field may be used to track lesions across several pictures in the dataset.Figure (7) shows a selection of skin cancer photos from the collection.

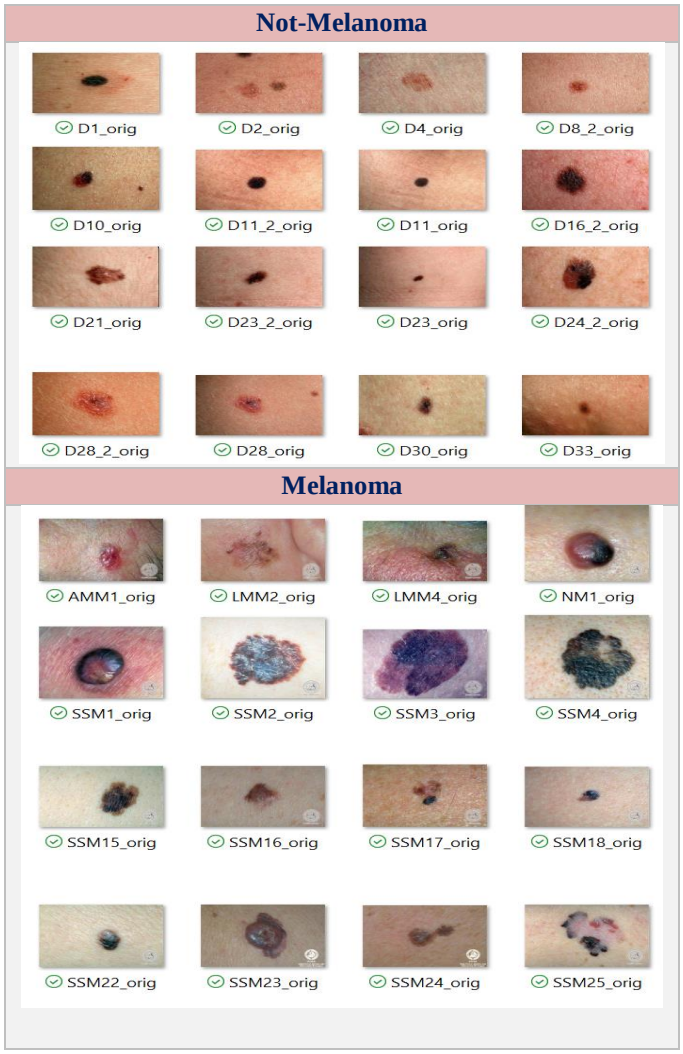

Figure (7) sample of dataset skin cancer

B. preprocessing stage

It's general known that the most important image processing methods can't start until the pre-processing is finished. Its goal is to make the target image better so that additional processing can produce better results. At this step, the models are subjected to the following preprocessing procedures: Remove the noise from the image using a medium filter con-tained in the database.

i. Medium Filter

Because use images are usually taken in low-light and high-noise environments, the recommended preprocessing

JOURNAL OF ALGEBRAIC STATISTICS
Volume 13, No. 2, 2022, p. 3072-3083
https://publishoa.com
ISSN: 1309-3452

method includes an intermediary filter to effectively show image data. Because the image may contain distracting pixels, an average filter is used. After applying the average filter, the image became smoother. The average filter used in this study

$$median\,[S(x)+A(x)] \neq median\,S(x)+median\,A(x) \quad (9)$$

S(x) and A are the operations on two pictures (x). The information on the several channels is regarded as having minute and exact details. The median is just the average of all the pixels in the local vicinity's standards. Median filtering is very good at ignoring different forms of noise.

C. Segmentation Stage

Segmentation can be done on the preprocessed picture. The preprocessed picture can be used as an input to the segmentation step. Watershed segmentation is used to assess the ridges, and the final result is displayed. The arithmetical system hypothesis is used to segment images via watershed segmentation. The watershed technique uses an intensity-based topographical representation in which luminous pixels indicate elevated distances or 'hills,' while unilluminated pixels correspond to 'valleys,' allowing the route of a falling raindrop to be verified. Watershed edges are the partition borders of 'prov-inces of attraction' of water droplets (or the limitations of catchment basins). The flooding alteration of the watershed approach is akin to the capture of assistance in a lake inundated from small holes. This version outperforms the traditional falling raindrop technique in a variety of conditions. The topographical representation is used in the watershed method. The basis of intensity, in which luminous pixels signify increased distance or 'hills,' and nonluminous pixels correspond to 'valleys,' allowing the passage of a falling raindrop to be verified. The distinct lines in the region of water drop captivation are known as watershed lines.' The flooding version of the watershed approach is equivalent to concentrating the discharge in a lake inundated from the smallest feasible space. In many cases, the flooding technique is more effective than the traditional falling raindrop method. The fundamental watershed rain-fall characteristics execution is used in these crucial phases to reach the least region by following the raindrop passage.

1. In many cases, the flooding technique is more effective than the traditional falling raindrop method. The fundamental watershed rain-fall characteristics execution is used in these crucial phases to reach the least region by following the raindrop passage..

2. Rerun the rainfall model on all surrounding pixels to check if there's another point where the area is decreased in a comparable way. If the minimum region is not met, a new streaming approach will begin with a minimum region designed for continuing streaming..

3. When different brands of waterholes are concerned about merging, a 'dam' is built to prevent the merging. While the streaming process reaches the inclusive limit, the dam limits are finally formed. The watershed lines represent the barrier constraints at this time.

D. Feature extraction

ORB interest Point Detection and point feature provided information on the features. We choose the most significant features utilizing a set of criteria and thresholds, and then we return all aspects that reflect the most essential properties of our object of interest, as well as the original image. Feature descriptors, also known as data carrier features, are then derived from the pixels that surround a point of interest. Pixels are properties that are defined by the position of a single point. This determines the center positioning of neighboring pixels. Finally, we arrive to the most evocative description. POI's skin cancer representation points are referred to as a result of download information that may be recognized and identified. Finally, it compares features from the first group of coronavirus disease images to the second set of characteristics in the original image. Indicators for features that are compatible with the pair of features are returned by the matching step.

JOURNAL OF ALGEBRAIC STATISTICS
Volume 13, No. 2, 2022, p. 3072-3083
https://publishoa.com
ISSN: 1309-3452

E. Skin Cancer Classification utilizing SVM

The next stage is classification, which splits the pictures into benign and malignant groups. A normal picture is referred to as "benign," but a malignant image is referred to as "mel-anoma." There are several plans from which to pick. Vector-Supporting Machine (SVM) For both classification and regression problems, the supervised machine learning approach Support Vector Machine (SVM) is used. It is, nonetheless, frequently used in classification issues. Design each data point as a place in a structural hole (where n is the number of characteristics), with the value of explicit correlations showing the importance of each attribute. Support Vectors are just the correlations of a number of tests. The front line that best divides the two classes is the Support Vector Machine (/).

SVM generation algorithm
Input: Data that has been trained and data that has been tested.
Output: Data that has been classified.
Step 1: The system is provided the data set.
Step 2: Based on the identified class, features and characteristics are categorized.
Step 3: Estimation of Candidate Support Value
Step 4: If the value of the instance is not null, repeat Steps 1–4 for all instances.
Step 4: Support Value is equal to the similarity of each attribute instance.
Step5: Calculate the Total Error Value.
Step 6: Estimate the decision value if any of the instances are less than 0.
Step 7:Support Value/Total Error = Decision Value
Step 8: Rep the procedures above until the container is emptied.
End If

5. Experimental Results

Skin cancer will be discovered at this point by passing through numerous steps of the suggested procedure, which will be explained below.

A. Preprocessing utilizing Median Filter

At this stage, the noise is eliminated, as shown below

Orginal image	*Preprocessing image*
	

Figure (8) Preprocessing for skin cancer Image

B. Segmentation stage

At this stage, segmentation of a skin cancer image model for the watershed method to an as shown in Figure(9).

Watershed Segmentation of skin cancer
Segmentation of Melanoma

JOURNAL OF ALGEBRAIC STATISTICS
Volume 13, No. 2, 2022, p. 3072-3083
https://publishoa.com
ISSN: 1309-3452

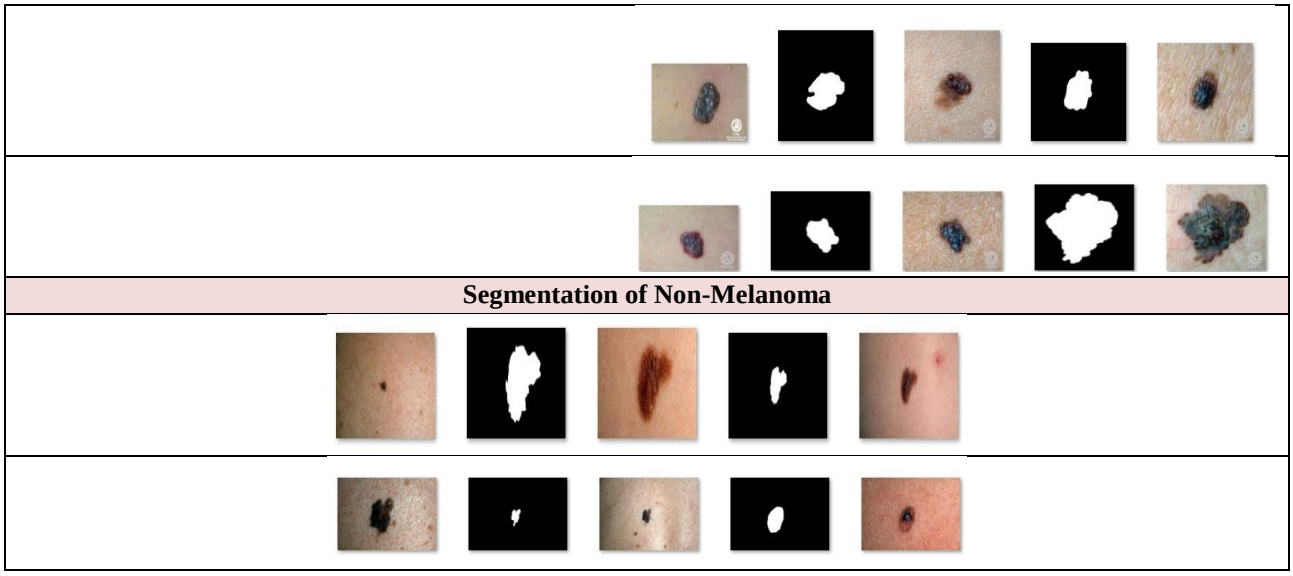

Figure (9) Segmentation of skin cancer

C.Feature Extraction utilizing ORB

At this stage, it is clarified how the feature extraction was calculated, as shown in Figure(10) and Table (1), (2).

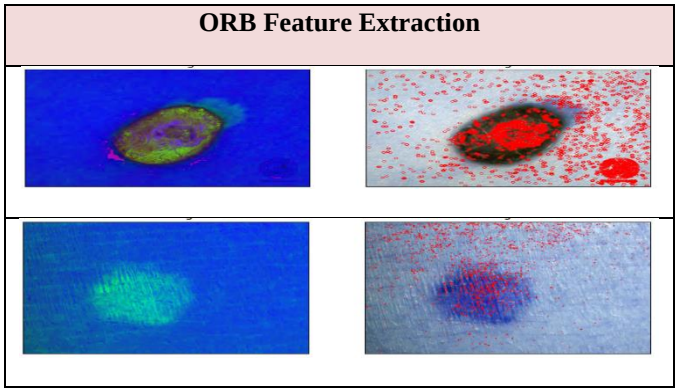

Figure (10) ORB Feature Extraction

Table (1) keypoint of *Melanoma*

Image Melanoma	*Threshold*	*Non-maxSuppression*	*neighborhood*	*Total Keypoints with non maxSuppression*	*Total Keypoints without non max suppression*
1	20	True	2	1444	3585
2	20	True	2	2784	4876
3	20	True	2	2564	3572
4	20	True	2	1348	3435
5	20	True	2	1098	2456
6	20	True	2	1508	2954
7	20	True	2	2098	3672

Table (2) keypoint of *Non-Melanoma*

JOURNAL OF ALGEBRAIC STATISTICS
Volume 13, No. 2, 2022, p. 3072-3083
https://publishoa.com
ISSN: 1309-3452

Image Non-Melanoma	*Threshold*	*Non-maxSuppression*	*neighborhood*	*Total Keypoints with non maxSuppression*	*Total Keypoints without non max suppression*
1	20	True	2	1943	2678
2	20	True	2	2421	3421
3	20	True	2	1425	2576
4	20	True	2	1778	3456
5	20	True	2	1661	3425
6	20	True	2	2008	3098
7	20	True	2	1473	3246

D.Classification utilizing SVM

Melanomas and non-melanomas can be classified by specifying their algorithm so that 30% of the test samples and 70% of the training samples are loaded into the databases. Specimens are graded by evaluating the diameter closest to the state of preparation. It then concludes with its own sample classification section. The SVM classifier extends this suggestion by grabbing the adjacent position by declaring the dominant direction signal. It is unique to choose values from ORB. After the accuracy of the system was calculated by utilizing the fixed measurement criteria which are Cofusion Matrix methods, accuracy, sensitivity, specificity, and giving remelting as shown in Table (3).

Table (3) Performance analysis of Skin Cancer

Parameters	*Classifier*
Accuracy	98%
Sensitivity	95%
Specificity	96%

6.. Conclusion

The method of segmentation and the way of grading melanoma are discussed in this study paper. The classification of introducing a image into the skin is divided. The ORB method may be utilized to dissect lesions on the skin by enhancing tightness by adding color, back-defining, separating, and finally removing strong characteristics. Finally, the collected database was utilized to simulate the system utilizing the SVM approach. The new classifiers technology was utilized to assess the incremental stage. SVM has several advantages, including being accurate and resilient even when the training sample is biased. Becautilize the convex problem is optimized, it delivers a one-of-a-kind solution. Out-of-sample generalization is good with SVMs. Becautilize its function is non-parametric and acts locally, SVMs have the freedom to pick the solvent separation threshold form, which does not have to be linear and does not even need to be the same for all data. The system's results show a high accuracy of 98%.

REFERENCES

[1] Barata, C., Celebi, M. E., & Marques, J. S. (2018). A survey of feature extraction in dermoscopy image analysis of skin cancer. IEEE Journal of biomedical and health informatics, 23(3), 1096-1109.

[2] Nasir, M., Attique Khan, M., Sharif, M., Lali, I. U., Saba, T., & Iqbal, T. (2018). An improved strategy for skin lesion detection and classification utilizing uniform segmentation and feature selection-based approach. Microscopy research and technique, 81(6), 528-543.

[3] Afza, F., Khan, M. A., Sharif, M., & Rehman, A. (2019). Microscopic skin laceration segmentation and classification: A framework of statistical normal distribution and optimal feature selection. Microscopy research and technique, 82(9), 1471-1488.

JOURNAL OF ALGEBRAIC STATISTICS
Volume 13, No. 2, 2022, p. 3072-3083
https://publishoa.com
ISSN: 1309-3452

[4] Ghalejoogh, G. S., Kordy, H. M., & Ebrahimi, F. (2020). A hierarchical structure based on a stacking approach for skin lesion classification. Expert Systems with Applications, 145, 113127.

[5] Afza, F., Khan, M. A., Sharif, M., Saba, T., Rehman, A., & Javed, M. Y. (2020, October). Skin lesion classification: an optimized framework of optimal color features selection. In 2020 2nd International Conference on Computer and Information Sciences (ICCIS) (pp. 1-6). IEEE..

[6] Kassem, M. A., Hosny, K. M., Damaševičius, R., & Eltoukhy, M. M. (2021). Machine learning and deep learning methods for skin lesion classification and diagnosis: A systematic review. Diagnostics, 11(8), 1390.

[7] Ray, P. J., Priya, S., Ashok Kumar, T., Nuclear Segmentation For Skin Cancer Diagnosis From Histopathological Images, IEEE Proceedings of 2015 Global Conference on Communication Technologies (GCCT), 2015..

[8] M.-L. T. Johnson and J. Roberts, "Skin conditions and related need for medical care among persons 1-74 years United States 1971-1974", Vital & Health Statistics, no. 212, 1978..

[9] Maglogiannis and C. N. Doukas, "Overview of advanced computer vision systems for skin lesions characterization" in IEEE Transactions on Information Technology in Biomedicine, 2009..

[10] Yang, J., Sun, X., Liang, J., & Rosin, P. L. (2018). Clinical skin lesion diagnosis utilizing representations inspired by dermatologist criteria. In Proceedings of the IEEE Conference on Computer Vision and Pattern Recognition (pp. 1258-1266).

[11] Sun, C., Hong, S., Song, M., Li, H., & Wang, Z. (2021). Predicting COVID-19 disease progression and patient outcomes based on temporal deep learning. BMC Medical Informatics and Decision Making, 21(1), 1-16.

[12] Alfed, N., & Khelifi, F. (2017). Bagged textural and color features for melanoma skin cancer detection in dermoscopic and standard images. Expert Systems with Applications, 90, 101-110..

[13] Afza, Farhat, Muhammad Sharif, Muhammad A. Khan, Usman Tariq, Hwan-Seung Yong, and Jaehyuk Cha. 2022. "Multiclass Skin Lesion Classification Utilizing Hybrid Deep Features Selection and Extreme Learning Machine" Sensors 22, no. 3: 799.

[14] Saba, T., Khan, M.A., Rehman, A., & Marie-Sainte, S.L. (2019). Region Extraction and Classification of Skin Cancer: A Heterogeneous framework of Deep CNN Features Fusion and Reduction. Journal of Medical Systems, 43.

[15]Ashfaq, Muniba & Minallah, Nasru & Ullah, Dr. Zahid & Ahmad, Arbab & Saeed, Aamir & Hafeez, Abdul. (2019). Performance Analysis of Low-Level and High-Level Intuitive Features for Melanoma Detection. Electronics. 8. 672. 10.3390/electronics8060672.